

# A Quadratic Actor Network for Model-Free Reinforcement Learning

Matthias Weissenbacher<sup>1</sup> and Yoshinobu Kawahara<sup>1,2</sup>

**Abstract**—In this work we discuss the incorporation of quadratic neurons into policy networks in the context of model-free actor-critic reinforcement learning. Quadratic neurons admit an explicit quadratic function approximation in contrast to conventional approaches where the non-linearity is induced by the activation functions. We perform empiric experiments on several MuJoCo continuous control tasks and find that when quadratic neurons are added to MLP policy networks those outperform the baseline MLP whilst admitting a smaller number of parameters. The top returned reward is in average increased by 5.8% while being about 21% more sample efficient. Moreover, it can maintain its advantage against added action and observation noise.

## I. INTRODUCTION

Underlying all reinforcement learning (RL) algorithms is the simple mechanism of receiving a reward feedback upon an interaction with the environment. This allows the algorithms to acquire sophisticated skills. Deep reinforcement learning has thus been successfully applied to a variety of tasks such as robotics [1] as well as board and video games [2]–[4]. In this work we focus on model-free algorithms which can be readily applied to various environments. In particular, online Actor-Critic methods for challenging settings with high-dimensional action and state spaces have recently gained a lot of attention [5]–[8]. The common perspective is that their success is owed to the use of deep neural networks which allow for high-capacity function approximations. The default policy network for the Actor is usually a Multi-Layer-Perceptron (MLP). The majority of the recent literature - with a few notable exceptions [9], [10] - attempts to improve learning results by altering the algorithm e.g. by modifying the loss function and interaction of the Actor and Critic. In contrast our angle is to study other policy networks with the aim of improving the general reward performance while reducing the number of trainable weights and being more computationally resource efficient. We achieve this by introducing a single layer quadratic neuron in between input and output in addition to the deep MLP in a network called Q-MLP (Quadratic-MLP), see fig. 1. The non-linearity of a conventional MLP is induced by the activation functions. In contrast, the Q-MLP allows for a direct approximation using the quadratic dependencies of the input as a first order optimisation problem. Thus naturally using quadratic layers one gains expressive advantages [11]. We introduce the Q-MLP only for the Actor network while we do not alter the Critic network i.e. we use a conventional MLP for the latter. For our empirical tests we focus on the two following state-of-the-art model-free

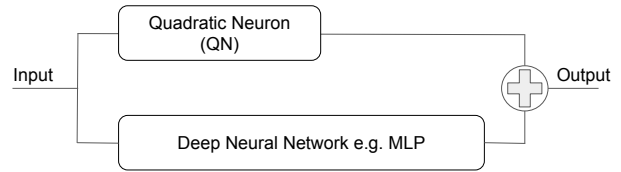


Fig. 1. Quadratic neuron connecting input and output in a single layer additively to a deep neural network architecture in our study given by a MLP.

algorithms: SAC [12] and TD3 [8]. Our source code as well as the raw data for our main results can be found online<sup>1</sup>. Let us emphasize that we do not modify the hyperparameters of the TD3 and SAC algorithm to accommodate for the Q-MLP actor policy. Regardless, we find a benefit across almost all tasks. The top returned reward for the TD3 is in average increased by 8.9% while being about 29.98% more sample efficient. The found improvements for the SAC algorithm are more moderate: 2.7% and 12.3% for top returned reward and sample efficiency, respectively. These numbers can be improved when relaxing the condition of reducing the number of weights of the Q-MLP in comparison to the MLP. E.g. we show that in the case of the Ant-v3 environment the benefit doubles from  $\sim 16\%$  to  $\sim 33\%$  for the top reward and from  $\sim 40\%$  to  $\sim 60\%$  for the sample efficiency compared to the MLP when increasing the number of weights of the quadratic layer. Moreover, it is worth noting that the benefit over the conventional MLP is maintained when action or observation noise is added.<sup>2</sup> For specific setups we even improve the noise robustness compared to the MLP. Noise robustness of deep neural nets is crucial for Sim2Real transfer, see e.g. [13] for a review. In particular, let us emphasise that our method does not require domain randomisation [14], [15].

Let us comment on another angle under which one may view our proposal. Reduction techniques of fully-connected neural networks to sparser representations with similar output performance have been widely investigated [16]–[20]. Those are mostly found in supervised learning research. The lottery ticket hypothesis states that “dense, randomly-initialized, feed-forward networks contain subnetworks that ... reach test accuracy comparable to the original network” [20]. The degrees of freedom of function approximation of the the Q-MLP are contained in a more parameter extensive MLP which naturally incorporates quadratic dependencies over the

<sup>1</sup> RIKEN Center for Advanced Intelligence Project, Japan

<sup>2</sup> Institute of Mathematics for Industry, Kyushu University, Japan

\*Equal contribution

<sup>1</sup>[https://github.com/matthias-weissenbacher/Quadratic\\_MLPs\\_in\\_RL](https://github.com/matthias-weissenbacher/Quadratic_MLPs_in_RL)

<sup>2</sup>Experiments for a smaller number of environments.

activation functions. Thus one may view the Q-MLP as a "sparser version" of the latter. One may thus consider our results as a step forward towards identifying a lottery ticket winner of neural networks in reinforcement learning.

The success of the Q-MLP may be attributed to the fact that it allows to propagate quadratic dynamic dependencies directly from input to output. In other words, the Q-MLP Actor Policy can thus adapt easily to gain potential benefits in exploring these quadratic directions. This seems beneficial in particular in an online reinforcement setting where dynamic exploration is the source for new data. Although not discussed explicitly in this work it is expected that our approach may as well lead to benefits in an offline reinforcement learning.

## II. RELATED WORK

To the best of our knowledge this work presents the first study of a quadratic layer in combination with a MLP as the policy network in the context of reinforcement learning. The standard policy network commonly used for the Actor in continuous control tasks is the Multi-Layer Perceptron (MLP). The non-linearity of deep neural networks as in the MLP is introduced by activation functions. Recently quadratic layers have been used in the context of categorical image classification in supervised learning [21]–[24]. We incorporate the quadratic neuron as a single unit between input and output additively to a MLP which is in contrast to [24].<sup>3</sup> Moreover, their study is restricted to supervised learning setups.

More relevant for us is the previously discussed architecture [9], [25] employed in the context of reinforcement learning. Their approach is conceptually analog to ours as their architecture is comprised of a linear module which directly connects the input state additively to the output state of a deep neural network i.e. the MLP, see fig. 2. The authors refer to this architecture as "structured control nets". In other words, the authors split the policy network into linear and nonlinear components where the latter is given by a MLP. This is in contrast to our approach where the quadratic neuron layer does not admit any linear components but is of quadratic order instead, see fig. 1. Moreover, it is worth emphasizing that as the quadratic neuron uses a quadratic function approximation it carries more complexity. Lastly, we allow for activation functions i.e.  $\tanh$  to act upon the sum of the quadratic neuron and the MLP output. Due to the similarity to [9] we provide

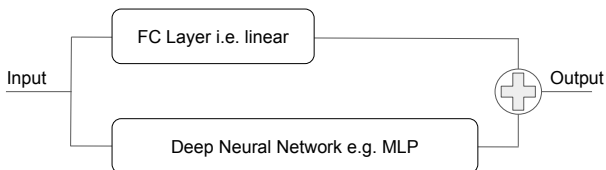


Fig. 2. Linear neuron i.e. a fully connected (FC) layer connecting input and output in a single layer additively to a deep neural network architecture e.g. a MLP.

results on their architecture in the ablation study, see fig. 2.

<sup>3</sup>Another distinguishing minor feature contrasting our work from [24] is that we make use of activation functions in the final layer.

Moreover, we provide the ablation study for the case where a quadratic neuron and FC layer are present, see fig. 3. Lastly,

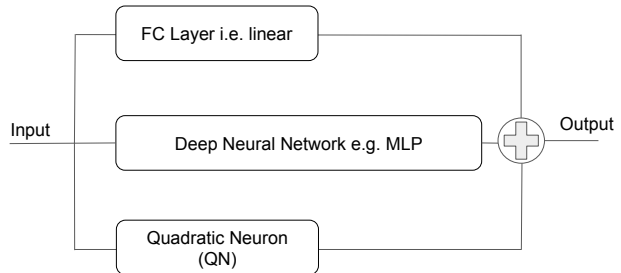


Fig. 3. Linear and quadratic neuron connecting input and output each in a single layer additively to a deep neural network architecture e.g. a MLP.

let us mention the idea of recurrent strategies in RL dates back two decades [26]. More recent advances build on the above strategy [10], [16]. Our results give comparable benefits while being supported by a much simpler architecture.<sup>4</sup>

## III. BACKGROUND

In this work we focus on two recent state-of-the-art model-free algorithms SAC [12] and TD3 [8]. SAC is an algorithm for soft Q-learning [12], [27], [28] which estimate a "soft Q-function" directly. The latter implicitly induces a maximum entropy policy. On the other hand the TD3 algorithm is the direct successor of DDPG [6], [29]. It owes its improvement over DDPG to the following three major changes: clipped double Q-Learning and delayed policy as well as target policy smoothing.

Let us remark that as a future extension of our present work it would be interesting to incorporate Q-MLP into other types of algorithms for scalable learning for continuous control problems such as Trust-Region Policy Optimisation (TRPO) [30] and its derivative class of Proximal Policy Optimisation algorithms (PPO) [31] as well as Maximum a Posteriori Policy Optimisation (MPO) [32], [33]. However, such a study is beyond the scope of this work.

### A. Preliminaries

Reinforcement learning algorithms train policies to maximize the cumulative reward received by an agent who interacts with an environment. The underlying setting is given by a Markov decision process  $(\mathcal{S}, \mathcal{A}, p, r, \gamma)$ , with  $\mathcal{S}$  being a set of states,  $\mathcal{A}$  the action space and  $p$  the transition density function. Moreover,  $\gamma$  is the discount factor and  $r$  the reward function. At any discrete time the agent chooses an action  $a_t \in \mathcal{A}$  according to its underlying policy  $\pi_\theta(a_t|s_t)$  based on the information of the current state  $s_t \in \mathcal{S}$ . The policy is parametrized by  $\theta$ . While the policy of the TD3 is deterministic i.e. it predicts a single action with probability one, the policy of the SAC algorithm is of stochastic nature. The parameters  $\theta$  naturally are the weights in the neural network function approximation of the Actor as well as the

<sup>4</sup>As our focus is on simple Actor policy architectures we do not consider LSTMs in the main scope of this work. And thus do not perform an empirical quantitative comparison of the Q-MLP with an LSTM architecture.

Critic. The agent i.e. the Actor-Critic is trained to maximize the expected  $\gamma$ -discounted cumulative reward

$$\mathcal{J}_\pi(\theta) = \mathbb{E}_\pi \left[ \sum_{t=0}^T \gamma^t r_\pi(s_t, a_t) \right], \quad (1)$$

with respect to the policy network parameters  $\theta$ .

#### IV. Q-MLP — QUADRATIC-MULTI-LAYER-PERCEPTRON

A quadratic neuron is a deep neural network layer that outputs a vector of quadratic monomials [34] constructed from the input e.g. for the input  $\mathbf{x} = (x_1, x_2, x_3)$  the output would be  $y = \Theta_{11}x_1^2 + \Theta_{12}x_1x_2 + \Theta_{13}x_1x_3 + \Theta_{22}x_2^2 + \Theta_{23}x_2x_3 + \Theta_{33}x_3^2$  where the  $\Theta$ 's are six trainable weights. The latter can be arranged in an upper triangular weights matrix  $\hat{\Theta}$  which allows one to generally express the action of the quadratic neuron as

$$y^f = \sum_{\substack{j=1 \\ j \geq i}}^N \sum_{i=1}^N \hat{\Theta}_{ij}^f x_i x_j = \mathbf{x}^T \cdot \hat{\Theta}^f \cdot \mathbf{x}. \quad (2)$$

Where  $f = 1, \dots, n_f$  with  $n_f$  the number of features of the quadratic neuron and  $\mathbf{x}$  a  $N$ -dimensional input vector. The trainable degrees of freedom of a quadratic neuron are given by the matrix elements of  $\hat{\Theta}^f$  i.e. its upper triangular components which are counted as

$$\frac{1}{2}N \cdot (N + 1) \cdot n_f. \quad (3)$$

One notes the  $\mathcal{O}(N^2)$  scaling which makes an efficient direct implementation of eq. (2) difficult for large hidden feature sizes. As proposed recently [24] one may simply take the common "square" of a single linear i.e. fully connected layer to approximate the degrees of freedom of eq. (2). This reduces the scaling to  $\mathcal{O}(N)$  as well utilizes the parallelisation benefits build into deep learning libraries [35], [36]. Thus we adopt the following implementation for the quadratic neuron in our work

$$y_f := \mathcal{Q}_f(\mathbf{x}) = \left( \sum_{i=1}^N \hat{\Theta}'_{fi} \mathbf{x}_i \right) * \left( \sum_{j=1}^N \hat{\Theta}''_{fj} \mathbf{x}_j \right). \quad (4)$$

where  $\hat{\Theta}'$  and  $\hat{\Theta}''$  are weight matrices. Note that the index  $f$  appears in both brackets in eq. (4) which denotes that the multiplication  $*$  is element-wise. Moreover, let us emphasize that the quadratic neuron in our neural network serves as a direct connection between input and output, see figure 1. Thus the implementation (4) is too restrictive as the input dimension is equal to the environments state vector and the feature dimensions equal to the one of the environments action state. Thus to allow for a higher number of trainable weights we choose the intermediate features size larger than the environments action state and introduce another linear layer as

$$y_a := \sum_{f=1}^{n_f := \text{hidden features}} \hat{\Theta}_{af} \mathcal{Q}_f(\mathbf{x}) + \mathbf{b}_a, \quad (5)$$

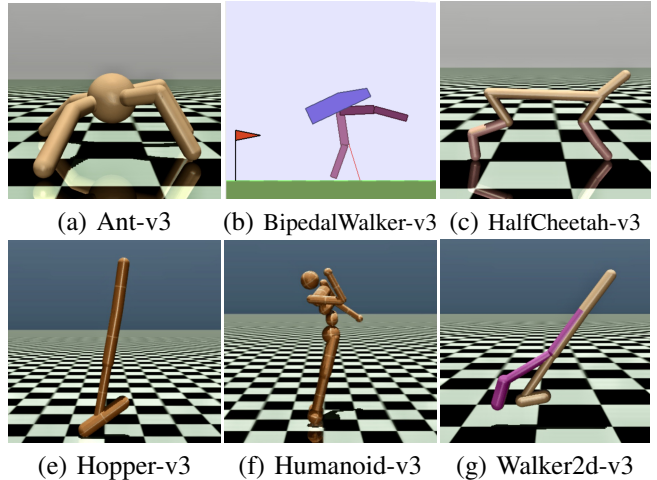


Fig. 4. Training environments (a) and (c)-(g) from MuJoCo and (b) from Box2D.

where  $\hat{\Theta}$ ,  $\mathbf{b}$  are the weight matrix and bias vector, respectively, while  $a = 1, \dots$ , number of action dimension of the environment. Eq. (5) simply represents another fully connected layer acting on (4). The crucial distinction to a MLP is that no activation function is used which would introduce additional non-linearities. Concludingly, (5) is of precisely quadratic order in the monomials of the input vector.

Our guiding principle is to reduce the number of weights compared to the three layer actor policy MLP network from [37] i.e. two hidden layers with hidden unit dimension 256 each. For the deep neural network part of our Q-MLP we choose the same three layer MLP architecture each with two hidden unit dimensions either  $n_h = 64, 128, 192$ . For the features for the quadratic neuron we are guided by the relation (3) to arrive at

$$n_f = \text{integer-part} \left( \frac{\kappa^2}{2} \cdot N \cdot (N + 1) \right), \quad \text{with } 0 < \kappa \leq 1, \quad (6)$$

where  $N$  is the input dimensions i.e. the observation space dimension of the environment. The expression (6) provides a convenient guiding principle for choosing the hyper-parameter  $n_f$  which served us well in achieving good empirical results without almost any hyper-parameter search.

## V. EXPERIMENTS

This section contains the empirical tests of our Q-MLP actor policy compared to the MLP baseline in V-B as well as an ablation study in subsection V-C.

### A. Training Environments & RL Algorithm

We exclusively focus on training environments with continuous state and action spaces. The selection for our empirical study consists out of five MuJoCo environments [38] namely: Ant-v3, Hooper-v3, HalfCheetah-v3, Humanoid-v3 and Walker2d-v3 and moreover the BipedalWalker-v3 from Box2D [39], see fig. 4. All experiments were conducted under the same conditions. The policies are evaluated every 5k time-steps averaged over ten episodes i.e. evaluation runs with different initial conditions. We train five different seed

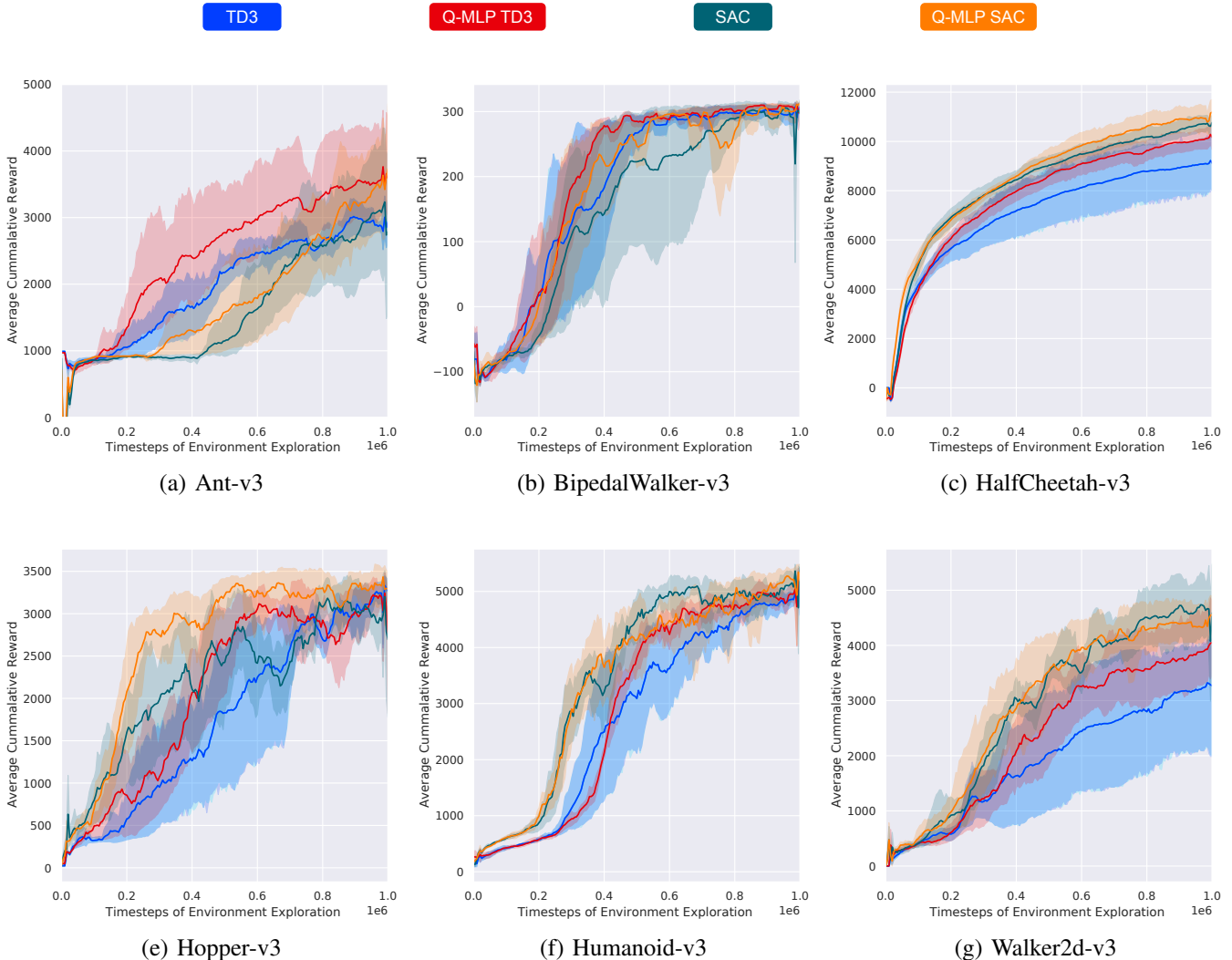


Fig. 5. Learning curves of environment (a)-(g) for both the TD3 and SAC algorithm. Mean and standard deviation averaged over five environment seeds, respectively. For better interpretability we have smoothened the plots uniformly by averaging over eight subsequent data points.

initialisation for the random seeds 0, 1, 2, 3, 4, respectively. The solid curves in all figures shows the average cumulative rewards per episode, and the shaded region represents the standard deviations. The implementation of the TD3 and SAC algorithms as well as hyper parameter settings are taken from [37]<sup>5</sup>. The latter is closely based on [8]<sup>6</sup> in the case of the TD3 algorithm and [40]<sup>7</sup> for the SAC algorithm. Thus these algorithms provide our baseline results which may be easily compared to the cited works.

### B. Q-MLP Performance on SAC & TD3

In this section we discuss our empirical results. The main results are given in fig. 5 which shows the comparison of the MLP to the Q-MLP tested with the TD3 and SAC algorithm, respectively. For the Q-MLP actor policy network we choose the hyper-parameters as in table 12. For the environments

<sup>5</sup><https://github.com/honghaow/FORK>

<sup>6</sup><https://github.com/sfujim/TD3>

<sup>7</sup><https://github.com/vitchyr/rlkit> and [https://github.com/denisyarats/pytorch\\_sac](https://github.com/denisyarats/pytorch_sac)

with small observation space dimension i.e.  $\mathcal{O}(10)$  such as HalfCheetah-v3, BipedalWalker-v3, Hopper-v3 and Walker2d-v3 (6) can be applied simply with  $\kappa = 1$ . For environments with large observation space dimension  $\mathcal{O}(100)$  such as Ant-v3 and Humanoid-v3 to arrive at a less weight extensive network architecture one must choose  $\kappa < 1$ . Note that for  $\kappa = 1$  eq. (6) provides the same order of degrees of freedoms as a honest quadratic neuron (3) where all the quadratic monomials are counted explicitly. For other hyper-parameters such as details of the MLP for the Critic network see the appendix.

In summary we conclude from fig. 5 that the Q-MLP results in performance gains across all environments and for both the TD3 and SAC algorithm. Let us emphasize that we do not modify the hyperparameters of the TD3 and SAC algorithm to accommodate for the Q-MLP actor policy. In table 6 we show the highest cumulative reward obtained averaged over the five training seeds for all environments and algorithms, respectively. We find that even for the choices



| Environment      | Q-MLP TD3       | TD3     | Improvement | Q-MLP SAC       | SAC            | Improvement |
|------------------|-----------------|---------|-------------|-----------------|----------------|-------------|
| Ant-v3           | <i>3847.40</i>  | 3317.29 | 15.98%      | <b>4027.65</b>  | 3423.88        | 17.63%      |
| BipedalWalker-v3 | <i>314.08</i>   | 308.48  | 1.82%       | <b>315.05</b>   | 314.46         | 0.19%       |
| HalfCheetah-v3   | <i>10295.54</i> | 9247.73 | 11.33%      | <b>11301.82</b> | 10884.99       | 3.83%       |
| Hopper-v3        | <i>3437.87</i>  | 3384.06 | 1.59%       | <b>3525.81</b>  | 3470.89        | 1.58%       |
| Humanoid-v3      | <i>5414.98</i>  | 5242.58 | 3.29%       | 5494.45         | <b>5508.70</b> | -0.26%      |
| Walker2d-v3      | <i>4159.95</i>  | 3485.84 | 19.34%      | 4651.67         | <b>4995.56</b> | -6.88%      |

Fig. 6. The table shows the top average reward for each environment and algorithm. Bold font highlights the best return reward while italic symbolizes the winner of the comparison of with and without quadratic neurons. The Q-MLP systematically outperforms the MLP. We separate the horizontal line for the Humanoid as well as Walker2d environment to highlight that no improvement for the Q-MLP SAC algorithm is found.

| Environment      | Q-MLP TD3   | TD3  | Improvement | Q-MLP SAC   | SAC  | Improvement |
|------------------|-------------|------|-------------|-------------|------|-------------|
| Ant-v3           | <b>575k</b> | 970k | 40.72%      | <i>845k</i> | 990k | 14.64%      |
| BipedalWalker-v3 | <b>740k</b> | 1M   | 26.00%      | <i>895k</i> | 970k | 7.73%       |
| HalfCheetah-v3   | <b>630k</b> | 995k | 36.68%      | <i>815k</i> | 975k | 16.41%      |
| Hopper-v3        | <i>720k</i> | 990k | 27.27%      | <b>515k</b> | 795k | 35.22%      |
| Humanoid-v3      | <b>865k</b> | 975k | 11.28%      | –           | –    | ~ 0%        |
| Walker2d-v3      | <b>565k</b> | 910k | 37.91%      | –           | –    | ~ 0%        |

Fig. 7. The table shows a comparison of the Q-MLP to the conventional MLP in terms of sample efficiency. Bold font highlights the best sample efficiency while italic symbolizes the winner of the comparison of with and without quadratic neurons. For the Humanoid and Walker2d for the SAC algorithm we omit the comparison as visual inspection of figures 5 (e) and (f) shows no quantitative difference.

$\kappa < 1$  performance benefits are obtained, see figure 5 and tables 6,7. This suggest that for those environments not all quadratic monomials weights need to be chosen independently for the actor to achieve high dynamic skills. Moreover, in table 7 we provide a quantitative measure for sample efficiency of the algorithms. Namely, the time-steps it takes to achieve the best reward (table 6) of the weaker environment in comparison between the MLP and Q-MLP. Let us illustrate this in an example. For the TD3 algorithm for the Ant-v3 environment the better reward is obtained by the Q-MLP, see table 6. Thus we compute how many time steps it takes both the TD3 as well as the Q-MLP TD3 algorithm to achieve the "weaker" top reward, i.e. the one obtained from the MLP without quadratic neurons. The time-steps are again averaged over the five seeds by using the mean values provided by the solid lines in the figures 5, respectively.

**Summary of main result:** In conclusion, we find a benefit across almost all tasks. The top returned reward for the TD3 is in average increased by 8.9% while being about 29.98% more sample efficient. The found improvements for the SAC algorithm are 2.7% and 12.3% for top returned reward and sample efficiency, respectively. This averages to **a total improvement of the cumulative reward of 5.8% while being 21.1% more sample efficient.**

Let us stress that the above performance measures for the Q-MLP can be improved by hyperparameter tuning. We will present details in the section V-C. In particular, we will find that improvements can be found by increasing the number of weights of the Q-MLP in compared to the study in figure 5 and tables 6 and 7. Moreover, there is a clear difference on the performance gain in between the SAC and the TD3 algorithm with the latter having a strongly increased benefit

of employing the Q-MLP network. As we do not perform any hyper-parameter tuning of the intrinsic values of the SAC nor the TD3 algorithm we cannot conclude on the origin of the difference.<sup>8</sup>

**Critical comment:** While we find that in general the performance benefit holds without much hyper-parameter tuning, for the Humanoid environment however the training results may vary. As the Humanoid is by far the most complex environment this caveat may be caused due to the rich state and action space. We traced the origin to the weight initializer which is Kaiming uniform by default [41]. A solution to enhance the training stability is to set the weight initializer of the quadratic neuron eq. (4) to zero i.e. for the weight matrices  $\hat{\Theta}' = \mathbf{0}$  and  $\hat{\Theta}'' = \mathbf{0}$  as well as the bias in (5).

**Noise Robustness:** We consider the TD3 algorithm for the Ant-v3 and HalfCheetah-v3 as those environments show a clear benefit in fig. 5 and the most complex environment the Humanoid-v3<sup>9</sup>. We find that the performance benefit of the Q-MLP is slightly improved further when adding action or observation noise at test time, see table 9 and 10. One concludes that for added action or observation noise the Q-MLP average benefit of 14.8% is improved to 19.7% and 16.3%, respectively. Lastly, it is worth noting that in particular for the Humanoid environment an increase in noise leads to a higher benefit of the Q-MLP.

<sup>8</sup>However, it is worth noting that our implementation of the Actor Policy networks uses a Xavier uniform weight initializer which is in contrast to the Kaiming uniform initializer used for the quadratic layer. It would be interesting to see in a future study if hyperparameter refinements such as the weights initializer for the Q-MLP SAC algorithm can lead to increased benefits across a wide range of tasks analog to the improvements found for the TD3 algorithm.

<sup>9</sup>With hyperparameters for Ant :  $n_h = 64$ ;  $\kappa = 0.25, 0.1$ , HalfCheetah:  $n_h = 192$ ;  $\kappa = 1.0$  and Humanoid:  $n_h = 192$ ;  $\kappa = 0.02^*$ .

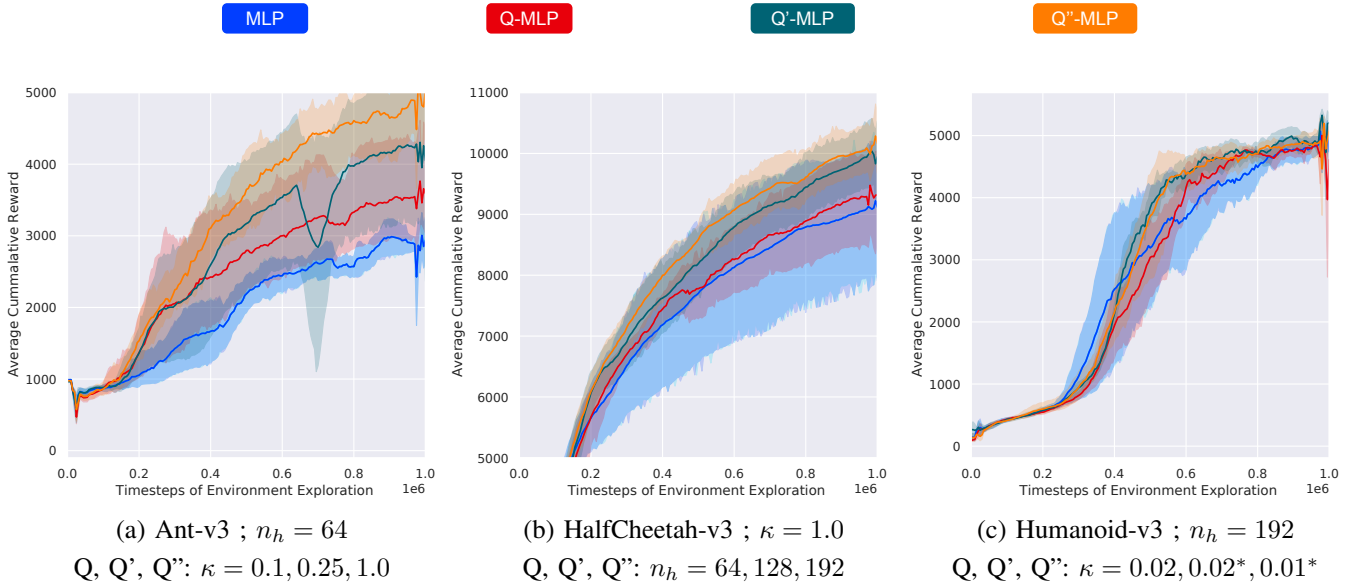


Fig. 8. Learning performance under hyperparameter changes of the Q-MLP i.e. its hidden state dimensions. The figure shows the learning curves for the TD3 algorithm of the Ant (a), HalfCheetah (b) and Humanoid (c) environment for different hyper-parameter settings denoted by Q, Q', Q''-MLP, respectively. In (a) we vary the  $\kappa$ -hyper parameter i.e. the hidden features  $n_f$  of the quadratic neuron while keeping  $n_h$  fixed. In (b) we keep  $n_f$  fixed and vary  $n_h$ . Lastly, in (c) we mainly compare initializing the weights of the quadratic neuron with value zero -denoted by the asterisk - to the default Kaiming uniform initializer. The precise hyper-parameter choices are found below the images in table. As for the MLP network we choose our default  $n_h = 256$ . The plot displays the mean and standard deviation averaged over five environment seeds, respectively. For better interpretability we have smoothed the plots uniformly by averaging over 12 subsequent data points.

| MLP vs. | Action Noise Added |       |       |       |       |
|---------|--------------------|-------|-------|-------|-------|
| Q-MLP   | 0.05               | 0.1   | 0.15  | 0.2   | 0.25  |
| 14.8%   | 18.3%              | 25.0% | 24.1% | 20.2% | 10.9% |

Fig. 9. Q-MLP performance gain over MLP for added action noise averaged over several environments. We evaluate the model of highest no noise performance for each seed then take the average. The displayed noise levels multiply a random action variable.

| MLP vs. | Observation Noise Added |       |       |       |       |
|---------|-------------------------|-------|-------|-------|-------|
| Q-MLP   | 0.01                    | 0.02  | 0.03  | 0.04  | 0.05  |
| 14.8%   | 13.7%                   | 16.3% | 18.7% | 17.6% | 15.0% |

Fig. 10. Q-MLP performance gain over MLP for added observation noise averaged over several environments. We evaluate the model of highest no noise performance for each seed then take the average. The displayed noise levels multiply a random observation variable.

### C. Ablation Study

In this section we perform an ablation study to compare the Q-MLP network to the alteration containing linear units see fig.'s 2 and 3. As well as discuss quantitative features of changes in the performance of the Q-MLP in regard to changes of the hyper-parameters  $n_h$  and  $\kappa$  i.e.  $n_f$ . For simplicity we restrict this study to only the TD3 algorithm in this section and to a reduced number of environments.

Let us start our study by discussing systematics of our approach in regard to changes of the hyper-parameters  $n_f$  and  $n_h$  as well as the weight initializers for the quadratic neuron layers, see figure 8.

**Fixed  $n_h$  and varying  $n_f$  &  $\kappa$ :** In figure 8 (a) we display

the learning curves for the Ant-v3 environment for increasing  $\kappa$  i.e.  $n_f$  and find that there is a direct positive correlation to the reward returned as well as the sample efficiency. In particular, we find that the benefit over the conventional MLP doubles from  $\sim 16\%$  to  $\sim 33\%$  for the top reward and from  $\sim 40\%$  to  $\sim 60\%$  for the sample efficiency when increasing the number of weights of the quadratic layer compared to the one used in table 6.

**Fixed  $n_f$  &  $\kappa$  and varying  $n_h$  :** In figure 8 (b) we display the learning curves for the HalfCheetah-v3 environment for increasing  $n_h$  and analogously find that there is a direct positive correlation to the reward returned as well as the sample efficiency.

**Initializer ablation study:** In figure 8 (c) we display the learning curves for the Humanoid-v3 environment. The focus is on the stability achieved by initializing the quadratic neuron weights with zero. For details see our comments earlier in the text. From this study we see that initializing the weights with zero not only leads to improved training stability over different hyperparameter choices. Furthermore, it slightly improves the sample efficiency.

Let us next turn our attention to the comparison of the Q-MLP network to the alteration containing linear units see figures 2 and 3. For all experiments we choose  $n_h = 64$  and  $\kappa = 1.0$ . The results can be found in figure 11.

**Main conclusion on linear units:** Our results figure 11 suggest that the benefit of using the linear unit is negligible and more likely leads to worse performance. Across the tasks (a) and (b) from fig. 11 one concludes that using the linear unit alone leads to a drop in the returned reward. In the

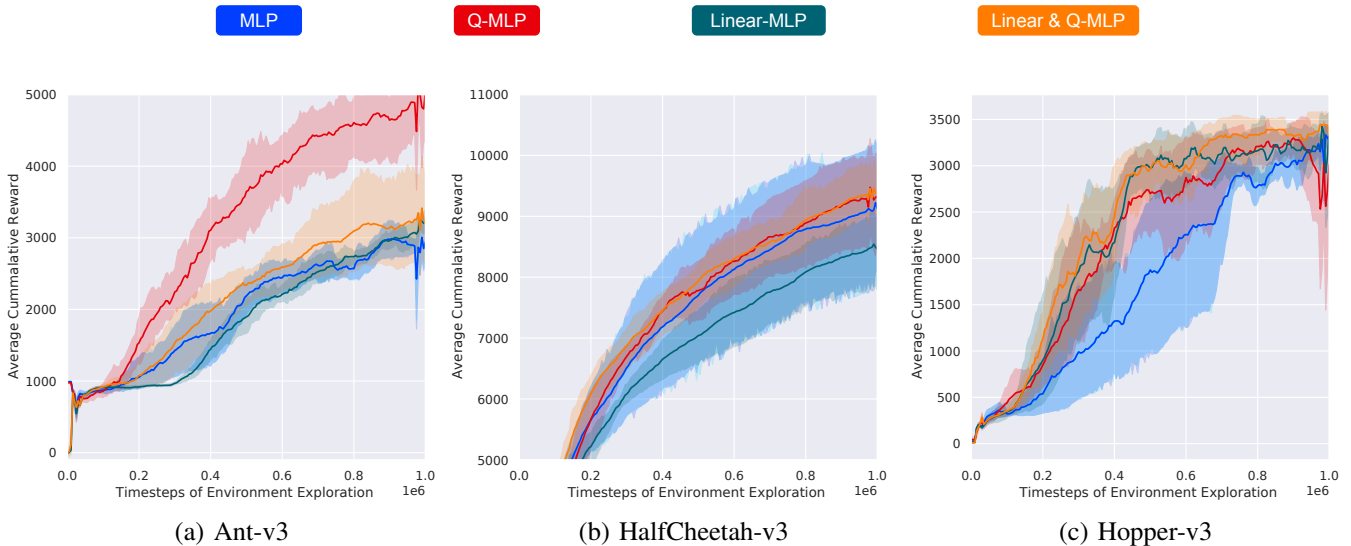


Fig. 11. Ablation study in regard to the network alteration containing a linear unit, see fig.’s 2 and 3. The plot shows the learning curves mean and standard deviation derived from five environment seeds, respectively. For better interpretability we have smoothed the plots uniformly by averaging over 12 subsequent data points.

HalfCheetah environment fig. 11(b) the network alteration with both a quadratic and linear neuron leads to a minor benefit over the Q-MLP alone. Whereas in the experiment fig. 11(c) the latter leads to a visible performance increase. In conclusion, for both alterations the downsides exceed the benefit. Moreover, let us emphasise that our results here do not reproduce the performance gains found in the original study of linear units [9]. It is our opinion that this is due to the fact that our TD3 and SAC algorithm produce significantly higher rewards as the ones in [9]. This is a critical point which we have observed using less sophisticated reinforcement learning algorithms: benefits due to changes in the actor policy which occur when using a weak RL algorithm often fade away when employing a state of the art algorithm. In other words, it is a much bigger challenge to have architectural modifications of the actor policy improve the performance of an already strong learning setup - such as the one used in this work -.

## VI. CONCLUSIONS

In this work we propose Q-MLP, a modification of the conventional MLP actor policy network to be used in Actor-Critic algorithms. Our contribution is the additional direct quadratic neuron connection between observation state input and action state output. Our empirical results derived by employing two state-of-the-art model-free reinforcement learning algorithms across six environments show performance improvements in terms of returned reward and sample efficiency. All while maintaining a smaller number of weights compared to the baseline provided by a conventional MLP actor policy network.

## APPENDIX

The neural networks are trained using Pytorch 1.7.1+cu110 and Python 3.8.7. The actor policy MLP as well as the

MLP part of the Q-MLP have two hidden layers with ReLU activation and hidden dimension units given in table 12, respectively. The final activation function of the Q-MLP is  $\tanh$ . For the critic network for both the TD3 as well as the SAC algorithm we use a MLP with two hidden layers with 256 units each and ReLU non-linearity. Moreover, the optimizer is Adam with learning rate  $3 \cdot 10^{-4}$ , discount factor  $\gamma = 0.99$ , replay buffer size  $1M$ , target update rate of  $5 \cdot 10^{-3}$  and a batch size of 100 for both the TD3 as well as SAC. For the TD3 we use a target update delay of 2, a policy noise of 0.2 with a noise clip of 0.5.

## ACKNOWLEDGMENT

We would like to thank Yoshiteru Nishimura for his technical assistance. The current work is, partly, supported by JSPS KAKENHI Grant Number JP18H03287 and JST CREST Grant Number JPMJCR1913.

## REFERENCES

- [1] T. Haarnoja, V. Pong, A. Zhou, M. Dalal, P. Abbeel, and S. Levine, “Composable deep reinforcement learning for robotic manipulation,” in *2018 IEEE International Conference on Robotics and Automation, ICRA 2018, Brisbane, Australia, May 21-25, 2018*. IEEE, 2018, pp. 6244–6251. [Online]. Available: <https://doi.org/10.1109/ICRA.2018.8460756>
- [2] D. Silver, A. Huang, C. J. Maddison, A. Guez, L. Sifre, G. van den Driessche, J. Schrittwieser, I. Antonoglou, V. Panneershelvam, M. Lanctot, S. Dieleman, D. Grewe, J. Nham, N. Kalchbrenner, I. Sutskever, T. Lillicrap, M. Leach, K. Kavukcuoglu, T. Graepel, and D. Hassabis, “Mastering the game of go with deep neural networks and tree search,” *Nature*, vol. 529, pp. 484–503, 2016. [Online]. Available: <http://www.nature.com/nature/journal/v529/n7587/full/nature16961.html>
- [3] Vinyals, Babuschkin, and Czarnecki, “Grandmaster level in starcraft ii using multi-agent reinforcement learning,” 2019.
- [4] M. Samvelyan, T. Rashid, C. S. de Witt, G. Farquhar, N. Nardelli, T. G. J. Rudner, C.-M. Hung, P. H. S. Torr, J. Foerster, and S. Whiteson, “The starcraft multi-agent challenge,” 2019.

| Environment      | Q-MLP TD3 |          |       |               | TD3   |         | Q-MLP SAC |          |       |         | SAC   |         |
|------------------|-----------|----------|-------|---------------|-------|---------|-----------|----------|-------|---------|-------|---------|
|                  | $n_h$     | $\kappa$ | $n_f$ | weights       | $n_h$ | weights | $n_h$     | $\kappa$ | $n_f$ | weights | $n_h$ | weights |
| Ant-v3           | 64        | 0.1      | 62    | <b>26.1k</b>  | 256   | 96.5k   | 128       | 0.1      | 62    | 47.7k   | 256   | 98.6k   |
| BipedalWalker-v3 | 192       | 1.0      | 300   | <b>58.2k</b>  | 256   | 73.2k   | 192       | 1.0      | 300   | 60.2k   | 256   | 74.2k   |
| HalfCheetah-v3   | 192       | 1.0      | 153   | <b>47.8k</b>  | 256   | 71.9k   | 192       | 1.0      | 153   | 49.9k   | 256   | 73.5k   |
| Hopper-v3        | 128       | 1.0      | 66    | <b>20.1k</b>  | 256   | 69.6k   | 128       | 1.0      | 66    | 20.6k   | 256   | 70.4k   |
| Humanoid-v3      | 192       | 0.02     | 28*   | <b>134.2k</b> | 256   | 166.7k  | 224       | 0.02     | 28*   | 164.5k  | 256   | 171.0k  |
| Walker2d-v3      | 64        | 1.0      | 153   | <b>11.8k</b>  | 256   | 71.9k   | 128       | 1.0      | 153   | 27.4k   | 256   | 73.5k   |

Fig. 12. Hyperparameter details of the actor policy networks. Hidden dimensions and total weight numbers of the Q-MLP and MLP neural networks used in the main study see figures 5 and tables 6 and 7. Note that the total number of weights is influenced by the observation and action space dimensions of the environment. Moreover, as the SAC algorithm admits a deterministic as well as stochastic policy each admitting the same number of weights displayed in the table, respectively. The asterisk symbolises that we have initialized the quadratic neuron with zero weights in contrast to the standard Kaiming uniform initializer [41] used in pytorch [35].

- [5] V. Mnih, A. P. Badia, M. Mirza, A. Graves, T. P. Lillicrap, T. Harley, D. Silver, and K. Kavukcuoglu, "Asynchronous methods for deep reinforcement learning," 2016.
- [6] T. P. Lillicrap, J. J. Hunt, A. Pritzel, N. Heess, T. Erez, Y. Tassa, D. Silver, and D. Wierstra, "Continuous control with deep reinforcement learning," 2019.
- [7] T. Haarnoja, A. Zhou, P. Abbeel, and S. Levine, "Soft actor-critic: Off-policy maximum entropy deep reinforcement learning with a stochastic actor," 2018.
- [8] S. Fujimoto, H. Hoof, and D. Meger, "Addressing function approximation error in actor-critic methods," in *International Conference on Machine Learning*, 2018, pp. 1582–1591.
- [9] M. Srouji, J. Zhang, and R. Salakhutdinov, "Structured control nets for deep reinforcement learning," 2018.
- [10] V. Liu, A. Adeniji, N. Lee, J. Zhao, and M. Srouji, "Recurrent control nets for deep reinforcement learning," 2019.
- [11] F. Fan, J. Xiong, and G. Wang, "Universal approximation with quadratic deep networks," *Neural Networks*, vol. 124, pp. 383–392, 2020. [Online]. Available: <https://www.sciencedirect.com/science/article/pii/S0893608020300095>
- [12] T. Haarnoja, H. Tang, P. Abbeel, and S. Levine, "Reinforcement learning with deep energy-based policies," in *Proceedings of the 34th International Conference on Machine Learning*, ser. Proceedings of Machine Learning Research, D. Precup and Y. W. Teh, Eds., vol. 70. International Convention Centre, Sydney, Australia: PMLR, 06–11 Aug 2017, pp. 1352–1361. [Online]. Available: <http://proceedings.mlr.press/v70/haarnoja17a.html>
- [13] W. Zhao, J. P. Queralta, and T. Westerlund, "Sim-to-real transfer in deep reinforcement learning for robotics: a survey," 2020.
- [14] G. Fernández, C. Togashi, D. Hong, and L. Yang, "Deep reinforcement learning with linear quadratic regulator regions," *ArXiv*, vol. abs/2002.09820, 2020.
- [15] M. Kaspar, J. D. M. Osorio, and J. Bock, "Sim2real transfer for reinforcement learning without dynamics randomization," *2020 IEEE/RSJ International Conference on Intelligent Robots and Systems (IROS)*, pp. 4383–4388, 2020.
- [16] Y. Lecun, J. Denker, S. Solla, R. Howard, and L. Jackel, "Optimal brain damage," in *Advances in Neural Information Processing Systems (NIPS 1989)*, Denver, CO, D. Touretzky, Ed., vol. 2. Morgan Kaufmann, 1990.
- [17] B. Hassibi and D. G. Stork, "Second order derivatives for network pruning: Optimal brain surgeon," in *Advances in Neural Information Processing Systems 5*, S. J. Hanson, J. D. Cowan, and C. L. Giles, Eds. Morgan-Kaufmann, 1993, pp. 164–171.
- [18] S. Han, J. Pool, J. Tran, and W. J. Dally, "Learning both weights and connections for efficient neural networks," 2015.
- [19] G. Hinton, O. Vinyals, and J. Dean, "Distilling the knowledge in a neural network," 2015.
- [20] J. Frankle and M. Carbin, "The lottery ticket hypothesis: Finding sparse, trainable neural networks," 2018.
- [21] F. Fan, W. Cong, and G. Wang, "A new type of neurons for machine learning," 2017.
- [22] Jiang, Yang, and Zhu, "Nonlinear cnn: improving cnns with quadratic convolutions," *Neural Comput & Applic*, no. 32, 2020.
- [23] F. Fan, J. Xiong, and G. Wang, "Universal approximation with quadratic deep networks," 2019.
- [24] Z. Xu, J. Xiong, F. Yu, and X. Chen, "Efficient neural network implementation with quadratic neuron," 2020.
- [25] K. He, X. Zhang, S. Ren, and J. Sun, "Deep residual learning for image recognition," 2015.
- [26] B. Bakker, "Reinforcement learning with long short-term memory," in *NIPS*, 2001.
- [27] K. Rawlik, M. Toussaint, and S. Vijayakumar, "On stochastic optimal control and reinforcement learning by approximate inference," 07 2012.
- [28] R. Fox, A. Pakman, and N. Tishby, "Taming the noise in reinforcement learning via soft updates," *ArXiv*, vol. abs/1512.08562, 2016.
- [29] D. Silver, G. Lever, N. Heess, T. Degris, D. Wierstra, and M. Riedmiller, "Deterministic policy gradient algorithms," in *Proceedings of the 31st International Conference on Machine Learning*, ser. Proceedings of Machine Learning Research, E. P. Xing and T. Jebara, Eds., vol. 32, no. 1. Beijing, China: PMLR, 22–24 Jun 2014, pp. 387–395. [Online]. Available: <http://proceedings.mlr.press/v32/silver14.html>
- [30] J. Schulman, S. Levine, P. Moritz, M. I. Jordan, and P. Abbeel, "Trust region policy optimization," 2017.
- [31] J. Schulman, F. Wolski, P. Dhariwal, A. Radford, and O. Klimov, "Proximal policy optimization algorithms," 2017.
- [32] A. Abdolmaleki, J. T. Springenberg, Y. Tassa, R. Munos, N. Heess, and M. Riedmiller, "Maximum a posteriori policy optimisation," 2018.
- [33] A. et al., "A distributional view on multi-objective policy optimization," in *Proceedings of the 37th International Conference on Machine Learning*, ser. Proceedings of Machine Learning Research, H. D. III and A. Singh, Eds., vol. 119. PMLR, 13–18 Jul 2020, pp. 11–22. [Online]. Available: <http://proceedings.mlr.press/v119/abdolmaleki20a.html>
- [34] M. Gupta, L. Jin, and N. Homma, "Static and dynamic neural networks: from fundamentals to advanced theory," 2004.
- [35] A. Paszke and e. a. Gross, "Pytorch: An imperative style, high-performance deep learning library," in *Advances in Neural Information Processing Systems 32*, H. Wallach, H. Larochelle, A. Beygelzimer, F. d'Alché-Buc, E. Fox, and R. Garnett, Eds. Curran Associates, Inc., 2019, pp. 8024–8035. [Online]. Available: <http://papers.neurips.cc/paper/9015-pytorch-an-imperative-style-high-performance-deep-learning-library.pdf>
- [36] M. Abadi, A. Agarwal, M. Devin, and e. a. Ian Goodfellow, "TensorFlow: Large-scale machine learning on heterogeneous systems," 2015, software available from tensorflow.org. [Online]. Available: <http://tensorflow.org/>
- [37] H. Wei and L. Ying, "{FORK}: A {for}ward-looking actor for model-free reinforcement learning," 2021. [Online]. Available: <https://openreview.net/forum?id=IXW6Sk1075v>
- [38] E. Todorov, T. Erez, and Y. Tassa, "Mujoco: A physics engine for model-based control," in *2012 IEEE/RSJ International Conference on Intelligent Robots and Systems*, 2012, pp. 5026–5033.
- [39] E. Catto, "Box2d, a 2d physics engine for games." 2011. [Online]. Available: <http://box2d.org>.
- [40] D. Yarats and I. Kostrikov, "Soft actor-critic (sac) implementation in pytorch," [https://github.com/denisyarats/pytorch\\_sac](https://github.com/denisyarats/pytorch_sac), 2020.
- [41] K. He, X. Zhang, S. Ren, and J. Sun, "Delving deep into rectifiers: Surpassing human-level performance on imagenet classification," 2015.
- [42] G. Brockman, V. Cheung, L. Pettersson, J. Schneider, J. Schulman, J. Tang, and W. Zaremba, "Openai gym," 2016.